MADRID
inter.noise 2019
June 16 - 19
NOISE CONTROL FOR A BETTER ENVIRONMENT

Microphone Array Deconvolution Methods for Efficient Aeroacoustic Testing in Wind Tunnels

Picard, Christophe[1] ; Lepercque, Fabien ; Le Magueresse, Thibaut ; Minck, Olivier
MicrodB,
28 chemin du petit bois, 69130 Ecully, France

Hallez, Raphaël[2]; Lanslots, Jeroen
Siemens PLM Software,
Interleuvenlaan 68, Leuven, B-3100, Belgium

ABSTRACT

Microphone array techniques are widely used in wind tunnels to help analysing aeroacoustic noise radiated by scaled models, for instance, airframe noise in aeronautics. Such techniques provide a view of the noise source mechanisms without perturbing the flow or the acoustic field at the source location. Next to the conventional beamforming method, deconvolution techniques such as CIRA or Clean-SC have the advantage to provide quantitative source information and improved resolution. However, they are typically much more demanding in terms of computational effort which makes it difficult to use them during the test campaign where time is limited. This issue can be solved by using optimized computation algorithms based on GPGPU (General-Purpose computing on Graphics Processing Units). This paper presents the approach and implementation strategy for accelerating calculation of deconvolution maps. Results are shown for an airframe noise case (Array Analysis Benchmark of the test case DLR 1 - DO-728 Aircraft Half Model in closed wind tunnel). Very high speed up can be achieved which makes it possible to analyse data right after the measurement and therefore gain efficiency in wind tunnel testing process.

Keywords: Aeroacoustics, Wind tunnel measurements, Microphone array technique, Deconvolution, Airframe noise
I-INCE Classification of Subject Number: 72

[1] christophe.picard@microdb.fr
[2] raphael.hallez@siemens.com

1. INTRODUCTION

Aeroacoustic measurements based on acoustic arrays in wind tunnels can provide a detailed understanding of complex noise sources. In particular for airframe noise in aeronautics, wind tunnel tests help to investigate new aircraft concepts, verify performance of innovative designs and validate prediction models. Indeed, thanks to increasing computational power, more and more CFD models are used in design phases, and wind tunnel testing is the ultimate way to validate these models long before the

aircraft can actually fly. However, wind tunnel testing is often very expensive and must be performed efficiently to get the most out of the limited testing time.

Microphone array techniques provide a considerable amount of data from which it is possible to extract valuable information on the origin of sound such as location or power of acoustic sources. The most common microphone array method is certainly the conventional beamforming algorithm (CBF [1], also known as “delay-and-sum” [2]) because of its simplicity, robustness and computational efficiency. However it suffers from a lack of resolution in the low frequency range and from the inability to properly quantify the source power, especially in the case of complex source distributions like those generally encountered in aeroacoustics. These drawbacks have been tackled in the 2000’s with advanced beamforming-based algorithms such as deconvolution techniques. In the field of experimental aeroacoustics in wind tunnel, the number of existing methods is important (Clean-PSF [3], DAMAS [4], Clean-SC [5] and SEM [6], and the many derived versions). All of these methods in fact share the same theoretical basis. Indeed the physical model is the same and the techniques only differ from the final inversion algorithm, while, in aeroacoustics, the model in general assumes an uncorrelated monopole distribution in free field [7]. These deconvolution methods however require long computation time which makes it difficult to use during the measurement campaign where time pressure is typically very high. This issue can potentially be solved by using optimized computation algorithms such as GPGPU (GPGPU (General-Purpose computing on Graphics Processing Units) and by using a dedicated testing platform for efficient data management and processing. This paper presents how such techniques have been implemented and the gain observed on an airframe noise test case.

Microphone array processing techniques are first presented. A deconvolution technique called CIRA [8][9] is compared with the well-known Clean-SC method. Implementation details calculation speed optimization based on GPGPU architecture are then presented. Finally, efficiency gains obtained with the industrial implementation of such techniques in a commercial platform are presented based on an experimental airframe noise case.

2. MICROPHONE ARRAY TECHNIQUES

2.1 General principles

Many acoustic imaging techniques have been developed over the past 30 years. These techniques have in common the formalization of the theoretical problem which is to estimate the position and power level of acoustic sources from pressure measurements on a microphone array.

The principle of identifying sources consists of placing a microphone array facing the object to study and try to locate the main noise areas through specific processing of microphone signals, based on a source model chosen a priori. For aeroacoustic applications, the usual hypothesis is to assume that the phenomena are well represented by a distribution of uncorrelated monopoles [7]. This can be justified by the fact that the pressure correlation scales are lower than the spatial resolution of the method in general. One then seeks the model adequacy to the measurement data.

One distinguishes far field and near field zones of the array (respectively Fraunhofer and Fresnel zones). It is admitted [7] that it is advantageous to measure a source in the near field of the array, in particular to overcome the background noise. The source emission is then spherical and one performs a focused array processing where the position of the source is sought, that is to say the emission center of the spherical wave. This model is the most commonly used (in aeroacoustics anyway) and usually provides interesting and useful results. But it must be noticed that this is an approximation of the

propagation model and that the differences between the actual acoustic propagation and the propagation model can result in errors, especially on the source amplitudes.

In practice, one chooses a region of the scan area, where the presence of sources is sought for. For practical reasons linked to mechanical design, one generally arrange the microphones on a plane. For a typical 2D configuration, an area of source point candidates is then defined in a plane parallel to the microphone array.

2.2. Expression of the direct problem

By solving the wave equation in the frequency domain or Fourier domain for a source in an open field and discretizing the solution, the complex pressure vector $\boldsymbol{P}$ ($M \times 1$) received at the M microphones of the array at frequency f can be expressed as:

$$\boldsymbol{P} = \boldsymbol{G}_j q_j, \quad \textbf{(Equation 1)}$$

where q_j is the complex amplitude of a source at point $\boldsymbol{\xi}_j$ and $\boldsymbol{G}_j$ is the Green function vector ($M \times 1$) in free space between the source and the microphones M at points $\boldsymbol{x}_i$, $i \in [1 \dots M]$. The frequency dependence of the equations is omitted in the notation of this paper.

In the presence of strong background noise perturbation, as often the case in aeroacoustics, it is wise to proceed with ensemble averages in the frequency domain, assuming stationarity property of signals. For this, one uses the cross spectral matrix (CSM) of the measured signals on the array, [] matrix of complex values, expressed as:

$$\boldsymbol{C} = \langle \boldsymbol{P}\boldsymbol{P}^* \rangle, \quad \textbf{(Equation 2)}$$

with $\langle \cdots \rangle$ designating the ensemble average and the superscript $\blacksquare^*$ being the Hermitian complex conjugate operator.

Applying this to (Equation 1), in the presence of N sources and assuming uncorrelated source model, i.e. incoherent sources, leads to the following expression of the modelled CSM:

$$\boldsymbol{C}_{mod} = \sum_{j=1}^{N} \boldsymbol{G}_j \boldsymbol{G}_j^* Q_j, \quad \textbf{(Equation 3)}$$

with Q_j being the power spectral density of the sources at each considered point $\boldsymbol{\xi}_j$. Methods considering other source models also exist, see [12] and [13] for a review.

2.3. Expression of the inverse problem

Starting from (Equation 3), the sound source identification consists in the estimation of the power spectral density of the sources knowing the measured CSM $\boldsymbol{C}_{mes}$ (measured pressure signals on the array). This is an inverse problem that can be solved using a classical optimization procedure. For that, an objective function - error function or cost function - is defined, traducing the adequacy of the model to the measurement data. A L2-norm is chosen here to quantify the difference between the measured CSM and the modelled CSM, i.e.:

$$\varepsilon = \|\boldsymbol{C}_{mes} - \boldsymbol{C}_{mod}\|^2 \quad \textbf{(Equation 4)}$$

The objective is then to minimize this cost function by considering its gradient regarding the unknown, i.e. searching an estimation of unknown Q_j satisfying:

$$\frac{\partial \epsilon}{\partial Q_j} = 0 \quad \textbf{(Equation 5)}$$

All L2-norm-based methods in the field have a formalization of the problem represented by the (Equation 4) and (Equation 5). What differentiates them lies in the optimization algorithm.

Conventional beamforming method and general principle of deconvolution methods are presented thereafter.

2.4. Conventional Beamforming method

The most commonly used method in the industry for the identification of acoustic sources is the conventional beamforming (CBF) for which an estimate of the power spectral density is searched for each source point scanned one after the other among the chosen set of candidate points. This means considering the following modelled CSM :

$$\boldsymbol{C}_{mod} = \boldsymbol{G}_j \boldsymbol{G}_j^* Q_j \quad \textbf{(Equation 6)}$$

Deriving the optimization procedure leads to the following estimate of the source power spectral density A_j at the considered scan point $\boldsymbol{\xi}_j$:

$$A_j = \boldsymbol{w}_j^* \boldsymbol{C}_{mes} \boldsymbol{w}_j, \quad \textbf{(Equation 7)}$$

where $\boldsymbol{w_j} = \boldsymbol{G_j} / \boldsymbol{G_j^*} \boldsymbol{G_j}$ is viewed as a spatial filter.

In the case of a unique real source at point $\boldsymbol{\xi}_j$, the linear regression estimate A_j is the best estimation of the power spectral density of the real source [7].

2.5. Deconvolution methods

The conventional beamforming method suffers from severe limitations. The beamforming process in fact performs a spatial convolution between the acoustic field generated by true sources and the spatial distribution of microphones. This gives a directivity function to the array (also called Point Spread Function, PSF), whose shape depends on the number of microphones, their spatial arrangement, the frequency and the relative position of the center of the array to the scan point. This property generates artefacts as main lobes, side lobes and grating lobes that pollute the resulting source map. These non-physical artefacts may render physical interpretation difficult. The PSF at point $\boldsymbol{\xi}_j$ due to a source at point $\boldsymbol{\xi}_k$ can be expressed as:

$$\mathrm{R}_{jk} = \left(\boldsymbol{w}_j^* \boldsymbol{G}_k \boldsymbol{G}_k^* \boldsymbol{w}_j \right) = \left\| \boldsymbol{w}_j^* \boldsymbol{G}_k \right\|^2. \quad \textbf{(Equation 8)}$$

It is then possible to express the CBF result A_j as a product of the array directivity pattern R_{jk} and the true power spectral density Q_k:

$$A_j = \mathrm{R}_{jk} Q_k \quad \textbf{(Equation 9)}$$

Considering all scanned points the CBF map result, $(N \times 1)$ vector **A,** is expressed as the product of the complete PSF, i.e. $(N \times N)$ matrix **R**, and the $(N \times 1)$ vector of source candidates **Q,** thus forming a second linear system (also called in the field as the DAMAS problem [4]):

$$\mathbf{A} = \mathbf{RQ}, \quad \textbf{(Equation 10)}$$

which requires a second inversion method of a linear system. The special feature of (Equation 10) thus obtained is that all terms of the linear system are real and positive. It can be shown that the positivity constraint has a strong regularizing effect and tends to foster sparsity of the solution. Thus it is expected to find equivalently a local minimum by means of any algorithm used in applied mathematics even without any penalty.

To overcome artefacts due to the directivity of the array, the deconvolution process consists of two steps: 1/ estimate the CBF result at each point of the chosen scan grid with (Equation 7) and 2/ estimate the source power density taking into account all the scanning points at the same time by solving (Equation 10).

2.5.1. CIRA

In this section, an algorithm called Constrained Iterative Restoration Algorithm (CIRA) is proposed. It results from image reconstruction [9] and is adapted to acoustic problems [8]. CIRA is an iterative optimization algorithm in the class of Gradient Descent associated with a positivity constraint. Indeed, in the present problem, the unknowns to be estimated are power spectral densities, which are therefore necessarily positive.

However solutions of Equation 10 can be negative. Thus, it is necessary to add a positivity constraint to the algorithm.
The pseudo-code of CIRA is written as following:

1. Source power spectral density at iteration $i+1$ is expressed by
$$\boldsymbol{Q}^{(i+1)} = \left(C_+\left(\boldsymbol{Q}^{(i)}\right) + \mu \cdot \boldsymbol{r}^{(i)}\right)$$
with μ being the convergence parameter.
2. Calculate the residue at iteration $i+1$
$$\boldsymbol{r}^{(i+1)} = \left(\mathbf{R}C_+\left(\boldsymbol{Q}^{(i+1)}\right) - \mathbf{A}\right)$$
with the positivity constraint $C_+(\blacksquare) = |\blacksquare|$ or $= 0$.
3. Loop to step 1 until convergence is reached, i.e. if either a maximum (user defined) number of iteration i_{max} is reached or if the following error is small enough
$$\mathrm{E}^{(i+1)} = \left|\mathrm{N}^{(i+1)} - \mathrm{N}^{(i)}\right|$$
with $\mathrm{N}^{(i+1)} = \left\|\boldsymbol{r}^{(i+1)}\right\|^2$ the quadratic norm of the residue.

The implementation in an industrial context of this type of algorithm requires a lot of attention in particular with regard to the initial conditions, the management of convergence (setting μ parameter here) and positivity constraint, and the output conditions of the algorithm. There are also other implementation tricks useful for aeroacoustics (CSM diagonal removal, consideration of convection effects on acoustic propagation) that are not detailed in this publication.

2.5.2. CLEAN-SC

The Clean-SC method introduced by Sijtsma [5] is one of the most popular deconvolution methods in the field of aeroacoustics. Compared to classical beamforming, this technique provides a significant extension of the dynamic range and a slightly better separation power. Moreover, source extension and acoustic reflection or scattering are accounted for, in the sense that all the energy that is coherent with a beamformed signal is attributed to one single point in the clean map, even if the actual sound propagation from the noise sources to the array microphones do not match to the steering vector of the beamforming.
The Greedy algorithm (L1-norm type) of Clean-SC is depicted as follow. Starting with a null clean map, the iterative procedure is the following [3]:

1. Calculate a source plot with classical beamforming from (Equation 7) - the "dirty" map - and initialize the degraded CSM $\boldsymbol{S}^{(0)}$ by the measured one $\boldsymbol{C}_{mes}$
2. Clean map update:
    a. Search for maximum peak location in the dirty map $\xi_{max}^{(i+1)}$ with power $P_{max}^{(i+1)}$
    b. Store power $P_{max}^{(i+1)}$ in the clean map at location $\xi_{max}^{(i+1)}$
3. CSM cleaning:
    a. Compute the coherent steering vector $\boldsymbol{h}^{(i+1)}$ using the (degraded) CSM and the focused signal in $\xi_{max}^{(i+1)}$
    b. Compute the CSM induced by the source in $\xi_{max}^{(i+1)}$: $\boldsymbol{C}^{(i+1)} = P_{max}^{(i+1)}\boldsymbol{h}^{(i+1)}\boldsymbol{h}^{(i+1)}$
    c. Compute the degraded CSM $\boldsymbol{S}^{(i+1)} = \boldsymbol{S}^{(i)} - \boldsymbol{C}^{(i+1)}$.
4. Loop to step 1 for next iteration until the degraded CSM energy stops decreasing.

Clean-SC is computationally more efficient than CIRA particularly because it does not require to perform time-consuming operations with large matrix $\mathbf{R}$.

3. EFFICIENT IMPLEMENTATION OF DECONVOLUTION METHODS

3.1. Description of the AeroAcoustic Analysis Tool

To address the need for microphone array analysis in wind tunnels, Siemens and its partner MicrodB, have developed dedicated measurement and processing capabilities for efficient wind tunnel testing. It consists of the following main blocks:

- Instrumentation management for microphone array based on the Simcenter Testlab platform,
- Data acquisition systems based on the Simcenter SCADAS platform connected to the centralized data storage network,
- Measurement management system, which allows the operator to control the acoustic measurement, is equipped with multiple visualization systems to allow acoustic engineers to monitor the array measurement and online analysis,
- Post-processing systems for online or offline processing and analysis.

The aeroacoustic analysis software suite allows to perform all steps of the measurement from test setup definition to data collection and analysis. Case-by-case analysis and comparison can be performed by displaying the source maps on 2D or 3D geometries. It allows to make spectral calculations in fine and in third octave bands. It also allows to take into account the convection effect of acoustic waves by the flow and features a module for automated analysis and reporting including calculation of spatially integrated spectra from source maps.

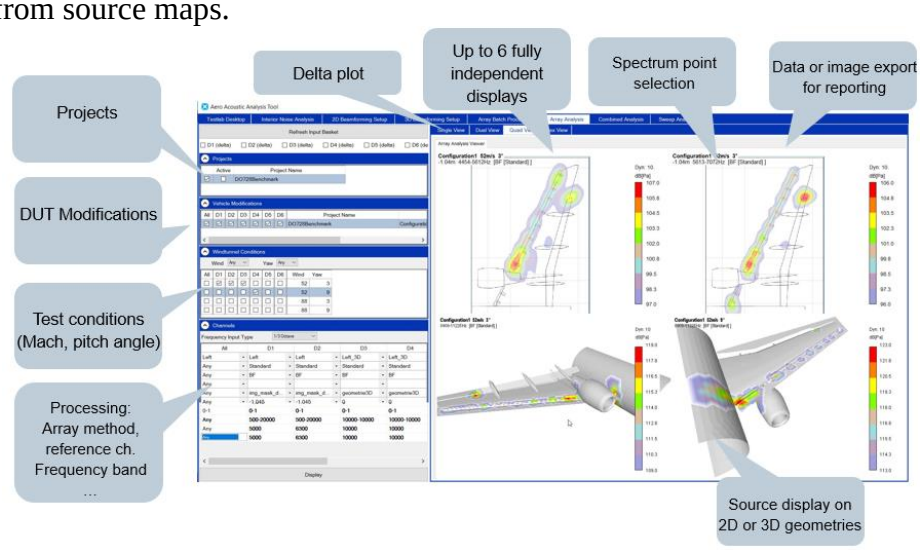

Figure 1 – Data selection view of the aeroacoustic processing software developed for productive wind tunnel testing

Indeed, during wind tunnel campaign, a large number of measurements are required (variation of parameters such as flow velocity, angle of attack, or different geometrical configurations). A large volume of measurement data is then produced and it is essential to have a robust, powerful post-processing tool capable of systematic analysis (so-called "batch" processing) rather than a case-by-case analysis. This efficient processing is carried out by using the “Array comparison and batch” capability which makes it possible to setup data for computation and process the data in a user-friendly and efficient manner (Figure 1). All computations are carried out using GPU (Graphics Processing Unit), using the graphics card rather than the usual processors (CPU). This allows to drastically reduce the calculation time. The achieved performance thus makes it possible to obtain a basic CBF map in a few seconds and a deconvolution map within the minute following the measurement.

3.2. GPGPU Programming

3.2.1. General consideration

The resolution of large and complex acoustic source localization problems often leads to a substantial demand for high-performance computing resources and parallelization strategies. Different parallelization strategies approach can be explored depending of the problem to be resolved and the target device. The recent technological advance of GPGPUs (General-Purpose computing on Graphics Processing Units) provides an interesting option for accelerating several acoustic sound source problem methods with inexpensive processing units. OpenCL and CUDA are the leading software frameworks that allow GPGPU to accelerate processing in professional applications. Instead of CUDA, the main asset of OpenCL framework is that it is open source and supports many GPU types (AMD, NVIDIA, INTEL…). For this reason, implementation of OpenCL kernel has been selected, which allows to handle the most complex and time-consuming algorithms, like Clean-SC. Moreover, once an OpenCL kernel is implemented, conversion to CUDA kernel is rather straightforward.

3.2.2. CLEAN-SC OpenCL kernel implementation

Clean-SC is a greedy algorithm and at every iteration, the source map is updated until the convergence criteria is reached. To get the best calculation time performance, all frequencies are computed in one batch. The computation procedure is depicted on Figure 2.

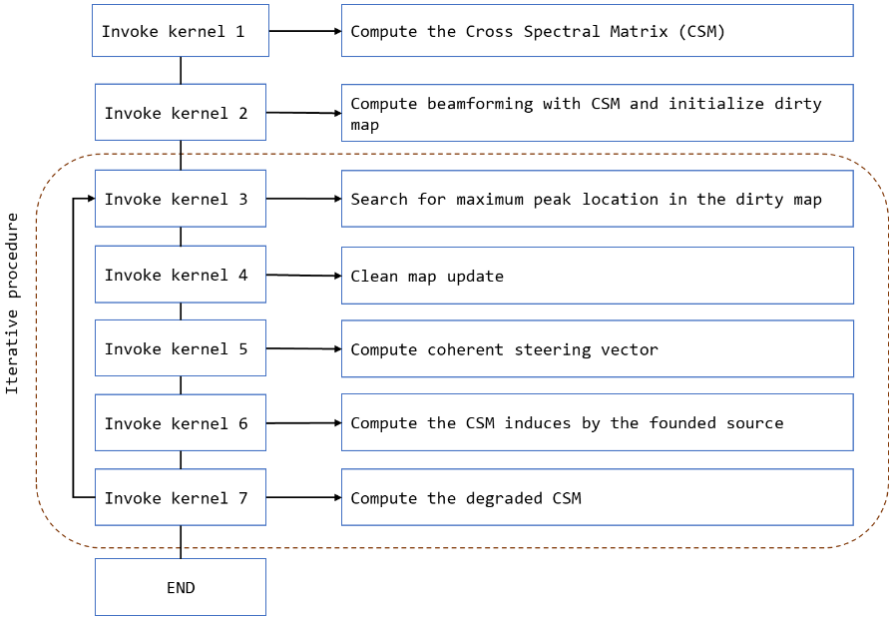

Figure 2 - CLEAN-SC calculation procedure on GPGPU.

4. VALIDATION TEST CASE

4.1. Test case description

The test case selected here is the AIAA array analysis benchmark case DLR 1, Aircraft Half Model in closed wind tunnel. This benchmark problem consists of a test configuration with a Dornier-728 half model of scale 1:9.24 in high-lift configuration (landing) placed in the center of the cryogenic wind tunnel at the DLR Kryo-Kanal Koeln (DNW-KKK). Figure 3 shows the test setup, see [10] and [11] for a more complete description of the test case.

Figure 3 – Left: Front view in the flow direction with the array mounted on the side wall and side view of the DO-728 half model in the test section,– Right: scanning grid of the source map calculations and microphone positions – source: [10] and [11].

The microphone array has a diameter of 1 m and is composed of 135 microphones arranged in spiral arms mounted onto the sidewall. The sampling frequency of microphone signals is 120 kHz.
The benchmark data is acquired for 9 couples of parameters: 3 model angles of attack (3°, 5° and 9°) and 3 free stream velocities (Mach numbers M=0.15, 0.2 and 0.25) during 30 seconds each. The region of interest of the half model, defined in the frame of the benchmark, is a 1.05 m x 1.45 m observation plane at a distance of y = 1.045 m (position of the wing root) from the microphone array.
Three grid resolutions of the source maps have been proposed in the frame of the benchmark: 1 cm, 2 cm and 5 cm leading to different numbers of equidistant scanning points respectively of 15476, 3869 and 660. In this paper, results for the case of M=0.25 (88m/s) and 3° angle are presented, for a grid of 2 cm resolution (3869 points).

4.2 Source localization results

Figure 4 shows localization maps for the 3 methods considered in this study – CBF, CIRA and Clean-SC. We observe that CBF works well from 3.15 kHz onwards. Spatial resolution increases with frequency while dynamic range decreases with frequency. It would require more microphones to improve the dynamic range at high frequency. Source localization is clearly aligned with aircraft model geometry. As it has been confirmed in the benchmark [11], sources are concentrated on leading edge slat track, especially near the engine, and secondary sources are found around the flap side edge whose contribution is growing with frequency. Clearly for aeronautics measurements in wind tunnel, CBF is a standard and robust processing method, it provides relevant and global initial results on source localization.

For a more precise source localization especially at lower frequency, deconvolution methods CIRA and Clean-SC must be used. All 3 methods are consistent and localize the noise sources at the same locations. Although CIRA brings some improvement compared to CBF, Clean-SC provides the cleanest maps, with sources having the size of the mesh (2x2 cm²). Tonal noise is observed in narrow-band spectrum around 6.8 kHz. It seems that CIRA is more sensible than Clean-SC to tonal noise (see 6.3kHz 3rd octave band). Moreover deconvolution methods are quantitative, providing acoustic intensity maps, as opposed to pressure noise maps with CBF.

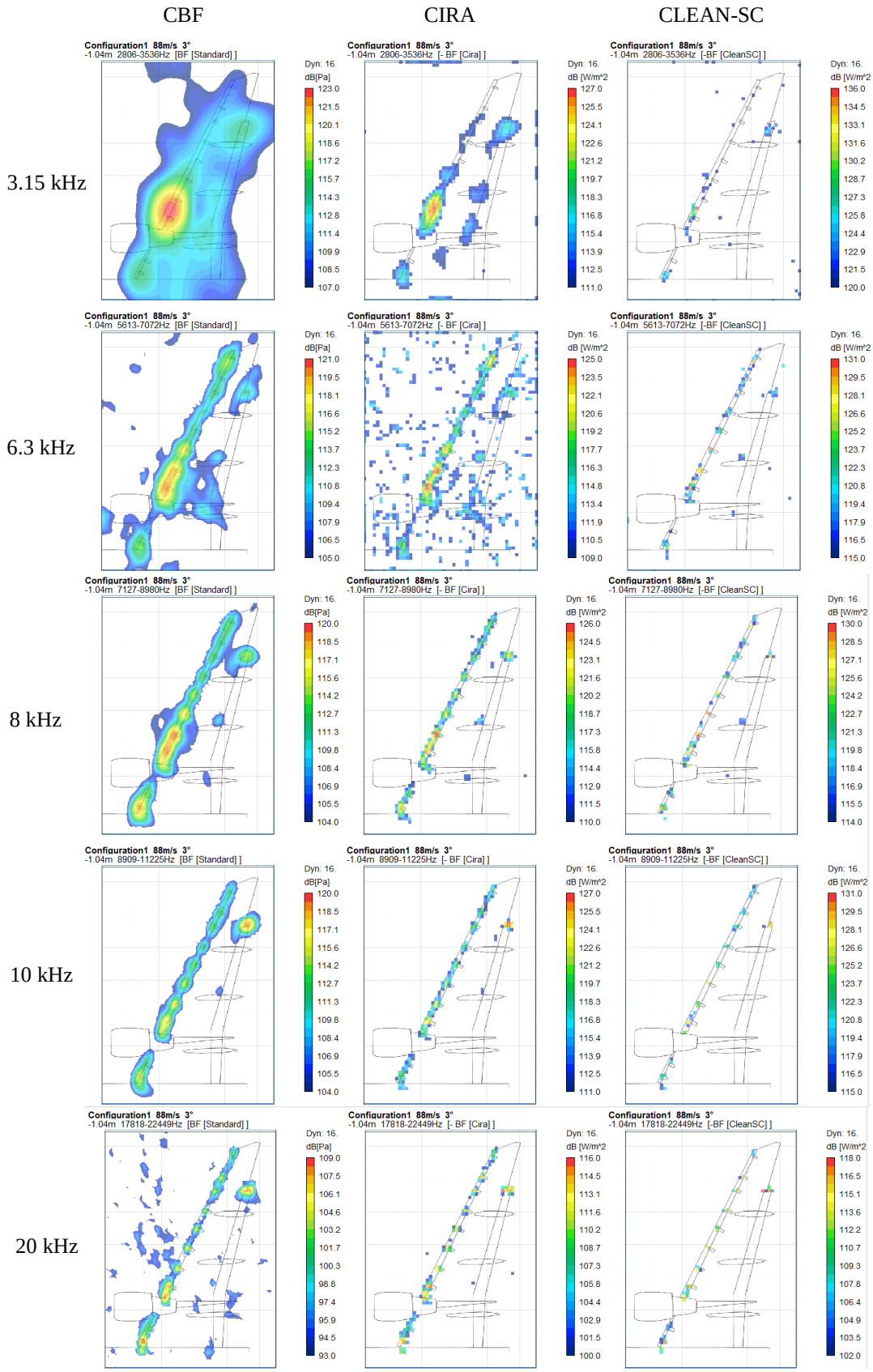

Figure 4 – Conventional beamforming and deconvolution results (CIRA and Clean-SC) for specific 3rd octave bands from 3.15kHz to 20 kHz, dynamic range 16 dB.

4.3 Source Quantification results

Figure 5 shows spatially integrated Sound Power Spectra. Similar spectrum shapes are observed with the 2 methods with some differences in levels: CIRA gives lower levels below 5 kHz, higher levels above and up to 1.1dB difference for power through total area. Total sound power level radiated by Flap is about 110 dB, for a total sound power of 120 dB.

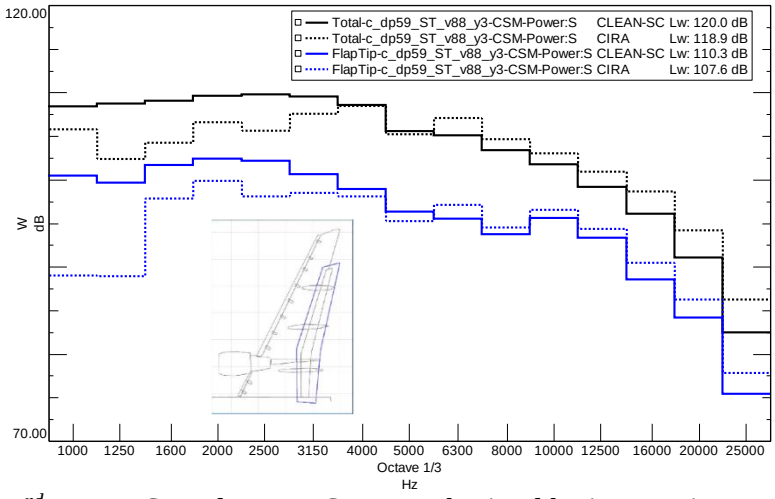

Figure 5 – 3rd octave Sound Power Spectra obtained by integrating source intensity over selected areas (total grid area – black and Trailing edge flap area - blue) – Clean-SC (continuous line) and CIRA (dotted line)

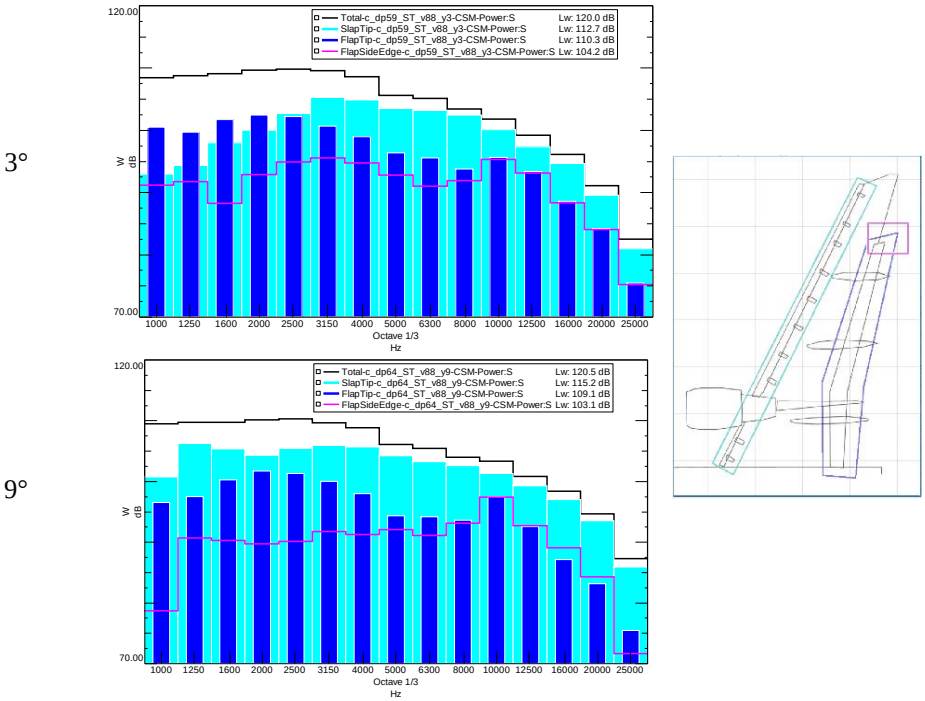

Figure 6 – Sound Power Spectra obtained by integrating CLEAN-SC source intensity over selected areas –angle of attack: 3° (top) and 9° (bottom)

Figure 6 shows radiated acoustic power when angle of attack is increased. For low angle of attack (3°), low frequency spectrum is dominated by the leading edge slats. Trailing edge flaps have higher contributions above 2.5kHz. For higher angle of attack (9°), leading edge flaps have the highest contribution through the entire spectrum, as

already observed earlier. Above 8 kHz, acoustic radiation from trailing edge flaps is essentially concentrated on the flap side edge.

4.4 Computational performance with GPU

Different grid sizes (from 4000 points to 100 000 points) have been tested to assess the performance of the Clean-SC GPU implementation in comparison with the CPU sequential version. For the tests shown below, the acoustic array is composed of 160 microphones, data is computed for 481 frequencies in one batch (from 1 kHz to 10.6 KHz with a resolution of 20 Hz). So, the final problem matrix to be resolved is of size : $number\ of\ frequencies \times grid\ size$. The tested GPU device is a Quadro P5000.

Excellent speed-up is observed with the GPU version, the best speedup gain being, on average, 54 time better than the sequential version for the tested grid sizes. More specifically, it is possible to compute large size problems with OpenCL GPU version in a very short time (less than 18 minutes with a 100 000 points grid size for about 500 frequencies) while it would take around 17 hours with the CPU sequential version.

Projected calculation time for the AIAA DLR1 case have been indicated in Figure 7 for a grid with resolution 2cm (3869 grid points) and 1cm (15 384 grid points). Calculation would take around 3 minutes for the OpenCL GPU kernel while it would take around 3 hours for the CPU sequential version on the fine grid.

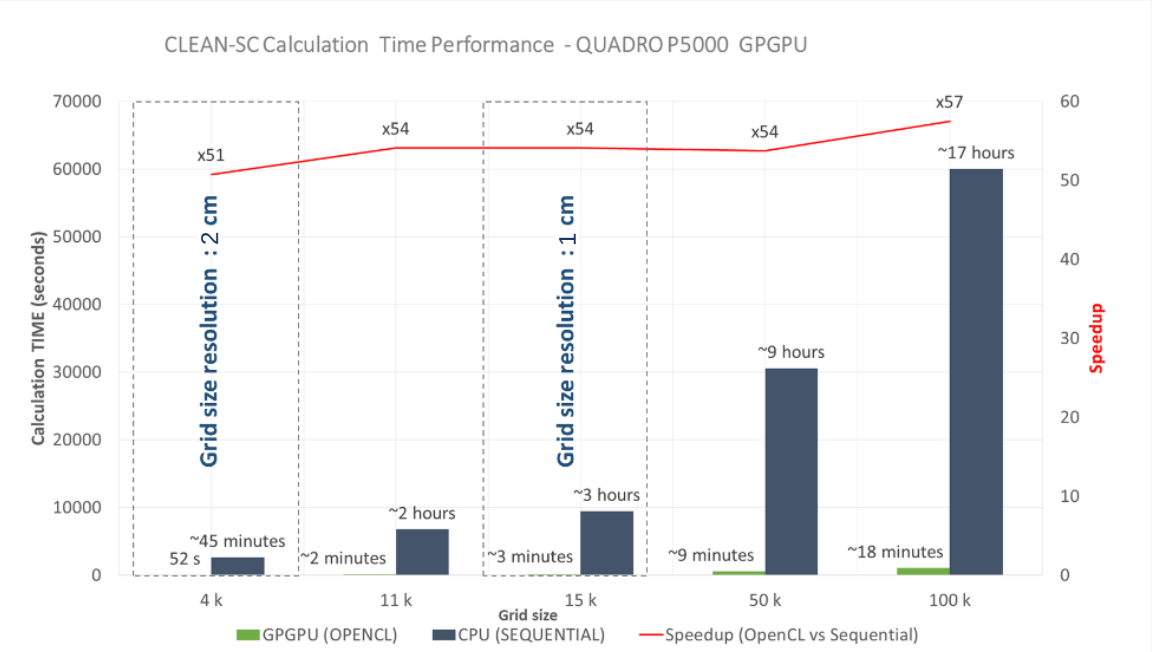

Figure 7 - Clean-SC calculation time performance for GPU versus CPU sequential implementation.

5. CONCLUSIONS

Microphone array methods and their implementation in commercial software for efficient aeroacoustic data processing in wind tunnels have been presented. For such applications, conventional beamforming is the basic localization method for immediate view of localization results during the test campaign. Clean-SC, well-known and well used method in the field, provides reference quantitative results, although sometimes a little bit too sparse. CIRA, intermediate method between conventional beamforming and Clean-SC provides complementary quantitative results, not so sparse (especially at low

frequency, i.e. CIRA is better adapted to spatially extended sources). Typical drawback of deconvolution methods lies in the high computational effort required. This issue has been solved by implementing efficient GPGPU techniques for solving the deconvolution problem. This allows to bring additional efficiency in wind tunnel aeroacoustic testing and to provide not only qualitative but also quantitative source information very quickly after the measurements.

6. ACKNOWLEDGEMENTS

The authors wish to acknowledge the array methods community for their input with regard to the value of this work, selecting datasets of interest, defining metrics, and providing feedback at various meetings and additionally, they wish to thank the team at DLR DNW-KKK facilities for their efforts in acquiring data for analysis.

7. REFERENCES

1. J. Billingsley and R. Kinns, *"The Acoustic Telescope"*, J. Sound Vib., vol. 48, (1976).

2. Don H. Johnson and Dan E. Dudgeon, *"Array Signal Processing: Concepts and Techniques"*, Prentice Hall, 1993. 0-13-048513-6, (1993).

3. R. Dougherty and W. Stoker, "Sidelobes supression for phased array aeroacoustic measurement", AIAA/CEAS 1998-2242, (1998).

4. Thomas F. Brooks and William M. Humphreys Jr., *"A Deconvolution Approach for the Mapping of Acoustic Sources (DAMAS) determined from Phased Microphone Arrays"*, 10th AIAA/CEAS Aeroacoustics Conference as Paper AIAA-2004-2954, (2004).

5. P. Sijtsma, *"CLEAN based on spatial source coherence"*, International Journal of Aeroacoustics, 6, 357-374, (2007).

6. Daniel Blacodon and Georges Elias, *"Level estimation of extended acoustic sources using an array of microphones"*, 9th AIAA/CEAS Aeroacoustics Conference as Paper AIAA-2003-3199, (2003).

7. G. Elias*, "Experimental Techniques for Sources Location"*, Von Karman Institute for Fluid Dynamics, VKI LS 1997-07, Aeroacoustic and active noise control, (1997).

8. B. Jacquet, *"Contribution à l'étude expérimentale et à la modélisation du bruit produit par l'impact d'un jet supersonique sur un obstacle"*, Thèse de Doctorat, Université de Technologie de Compiègne, (1994).

9. R. Schafer, R. Mersereau and M. Richards, *"Constrained Iterative Restoration Algorithms"*, IEEE 69(4), 432-450, (1981).

10. T. Ahlefeldt, *"Aeroacoustic measurements of a scaled half-model at high Reynolds numbers"*, AIAA Journal, vol. 51, no.12, pp 2783-2791, December, (2013).

11. C. J. Bahr, W. M. Humphreys, D. Ernst, T. Ahlefeldt, C. Spehr, A. Pereira, Q. Leclère, C. Picard, R. Porteus, D. J. Moreau, J. Fischer and C. J. Doolan, *"A comparison of microphone phased array methods applied to the study of airframe noise in wind tunnel testing",* 23rd AIAA/CEAS Aeroacoustics Conference. June 5 – 9, Denver, CO, USA, 2017, AIAA paper 2017–3718, (2017).

12. Q. Leclère, A. Pereira, C. Bailly, J. Antoni, and C. Picard, *"A unified formalism for acoustic imaging based on microphone array measurements",* International Journal of Aeroacoustics, Vol. 16, No. 4–5, pp. 431–456, SAGE Publications Ltd. London, United Kingdom, (2017).

13. A. Finez, C. Picard, T. Le Magueresse, Q. Leclère and A. Pereira, *"Microphone array techniques based on matrix inversion"*, VKI Lectures Series, STO-EN-AVT-287-05, (2017).